

# Photo and thermo luminescence studies of $\text{Sr}_2\text{SiO}_4: \text{Eu}^{3+}$ phosphor

B.S. Prathibha

*Department of Studies in Physics,  
University of Mysore, Manasagangothri, Mysore-570 006, India*

M.S.Chandrashekara

*Department of Studies in Physics,  
University of Mysore, Manasagangothri, Mysore-570 006, India*

B.M.Naghabhushan

*Department of Chemistry, M.S. Ramaiah Institute of Technology,  
Bangalore-560 054, India*

H.Nagabhushan

*Prof C.N.R Rao Centre for Advanced Materials,  
Tumkur University, Tumkur- 572 103, India*

**Abstract-**  $\text{Sr}_2\text{SiO}_4: \text{Eu}_{0.01}$  phosphor was prepared by solution combustion method and luminescent properties were investigated. The synthesized phosphor was characterized by XRD, FTIR, SEM, UV-Vis. PL studies on this phosphor was done with a view to obtain a white light emitting phosphor. The PL emission spectra are composed of peaks in all the three regions blue, green, and red. The TL glow curve shows that there is only one TL band peak at about 173 °C.

**Keywords –** Photoluminescence, Silicates, Combustion synthesis, Phosphor

## I. INTRODUCTION

Currently nanomaterials have become important within the field of luminescence because of enhanced optical, electronic, and structural properties than their bulk counter parts due to quantum size effect and an increased surface to volume ratio [1-2]. So nanomaterials exhibit excellent optoelectronic properties. With the advent of nanotechnology there is still a considerable amount of research for new nanocrystalline phosphor material with better luminescent properties.

Since from the last few years the research studies on phosphor doped with rare earth ions has made a rapid development. The intensity of white light emission can be enhanced by doping with rare earth. Rare earth doped phosphors have been used in almost all the fields because of their electronic and optical characters arising from 4f electrons. There are so many efficient rare earth ions which can be used as a dopant like Eu, Dy, Pr, etc but among these rare earth elements Eu will be the best dopant because it will exhibit two different valency trivalent and divalent. Because of these differences in valency the luminescent properties will also change [3-4]. The optical properties not only depend on the dopants it also depends on the host matrix. It has been reported that Eu exhibit favorable luminescence behavior in many matrices.

Recently more studies have been done by selecting  $\text{Sr}_2\text{SiO}_4$  host because of its excellent physical and chemical stability besides this it emits white light after absorbing UV radiation [5-6]. This inorganic phosphor has wide range of application because of its special properties like resistance to water, visible light transparency, wide energy band

gap, non toxicity, high temperature strength, high conductivity, multi colour phosphorence, and high resistance to alkali, acid and oxygen

Structure of  $\text{Sr}_2\text{SiO}_4$  is same as the structure of  $\text{Ba}_2\text{SiO}_4$ . As the  $\text{Sr}^{2+}$  ion has an effective ionic radius shorter than the  $\text{Ba}^{2+}$  ion and it is more similar to  $\text{Eu}^{3+}$  ionic radii, in this case the charge compensating mechanism could be better explained. It is having two alkaline earth sites which appear in equal amounts in the lattice. One site has 10 coordinations the other is surrounded by nine oxygen ions [7].

In order to use information about luminescence process of phosphors in various applications, the knowledge of defect centers and their distribution in the band gap of solid, reorganization of energy levels in the nanomaterials are very important. Very highly sensitive technique called TL has been used for the detection of such deeper or surface defects traps in insulators or semiconductor. These materials exhibit TL glow curves. These glow curve is nothing but the representation of TL emission as a function of temperature or time. The glow curve is related to trap levels lying at different depths in band gap between the conduction and the valence bands of a solid. Kinetic parameters are calculated from the glow curve [8].

Another important luminescence study is photoluminescence. Now a days the high energy efficiency of LED products attracts much attention of researchers who are interested in developing next generation lighting source because the substantial reduction in carbon related pollution is expected by reducing the number of power plants that consumes a lot of carbon based fuel [9]. Thus aim of our work is to design a phosphor with better luminescence efficiency.

So in present work we prepared  $\text{Sr}_2\text{SiO}_4$  doped with  $\text{Eu}^{3+}$  by combustion method. Reports says that now a day's silicates have been prepared by so many methods like solid state reaction, sol-gel, ball milling, flux fusion etc [10-13]. Since silicates have high melting points and glassy appearance synthesis of these silicates is tricky. The advantages of combustion method over the existing other methods is we can produce a homogeneous product in a short time without the use of expensive high temperature furnaces because this method makes use of the heat energy liberated by the redox exothermic reaction at a relatively low ignition temperature between metal nitrates and other fuels. More over this process is very simple and energy efficient [14].

Wei-Hsiang Hsu et al have prepared  $\text{Sr}_2\text{SiO}_4:\text{Eu}^{3+}$  [5], E.D. Bacce et al synthesized  $\text{Sr}_2\text{SiO}_4:\text{Eu}^{3+}$  and studied the luminescence behavior of this phosphor [7]. Less work has been done by selecting  $\text{Sr}_2\text{SiO}_4$  as host and doping Eu in  $3^+$  states. Thus the objective of this work is to report on the study of the luminescent behavior of  $\text{Eu}^{3+}$  -  $\text{O}^{2-}$  associates in  $\text{Sr}_2\text{SiO}_4$  doped with  $\text{Eu}^{3+}$ . But to the best of our knowledge this is for the first time we are reporting combustion synthesis of  $\text{Sr}_2\text{SiO}_4:\text{Eu}^{3+}$  using citric acid as fuel.

## II. EXPERIMENTAL

### A. Sample preparation

The powder sample with the general formula  $\text{Sr}_{1.99}\text{Eu}_{0.01}\text{SiO}_4$  phosphor was prepared by the solution combustion synthesis method. The starting materials were strontium nitrate, silica, europium oxide, citric acid. Citric acid was added as fuel.  $\text{Eu}_2\text{O}_3$  was dissolved in  $\text{HNO}_3$  to convert into  $\text{Eu}(\text{NO}_3)_3$  completely. The appropriate molar ratio of  $\text{Sr}(\text{NO}_3)_2$ ,  $\text{Eu}(\text{NO}_3)_3$ , citric acid were dissolved in a minimum amount of distilled water to obtain a homogeneous solution and stirred for few min. After completely stirring the mixture solution was introduced into a muffle furnace maintained at  $500^\circ\text{C}$ . Initially the solution boiled and underwent dehydration followed by decomposition with escape of large amount of gases then spontaneous ignition occurred and underwent smoldering combustion. The whole process was over with in less than 5 min, after the combustion the powder was cooled to room temperature, calcined at  $1100^\circ\text{C}$  for 3hr to get crystalline product.

### B. Methods of characterization

The phase identification of synthesized powder samples was carried out by using a Siemens d-500 XRD spectrometer ( $\text{Cu K}\alpha$ ,  $\lambda=1.541\text{\AA}$ ). The Fourier Infrared Spectroscopy was carried out by using a perkin elmer FTIR spectrometer. The PL emission and excitation measurements were carried out at room temperature using Horiba,

(model fluorolog-3) spectrofluorometer using 450 W Xenon as excitation source. Thermally stimulated luminescence measurements were carried out using TLD reader (Nucleonix, India) at a temperature of 300°C under a linear heating rate of 5°C/S.

## II. SAMPLE CHARACTERIZATION

### *Powder X-ray diffraction (PXRD)*

The powder XRD pattern of  $\text{Sr}_{1.99}\text{Eu}_{0.01}\text{SiO}_4$  phosphor is as shown in the Fig 1. Powder XRD pattern shows that the phosphor synthesized is crystalline and single phase. All the reflections were indexed according to the standard pattern of orthorhombic  $\alpha\text{-Sr}_2\text{SiO}_4$  available in JCPDS No 39-1256. No other phase was identified indicating that the doping  $\text{Eu}^{3+}$  was incorporated into the matrix lattice, rather than forming new phases beside the host material in the synthesis process

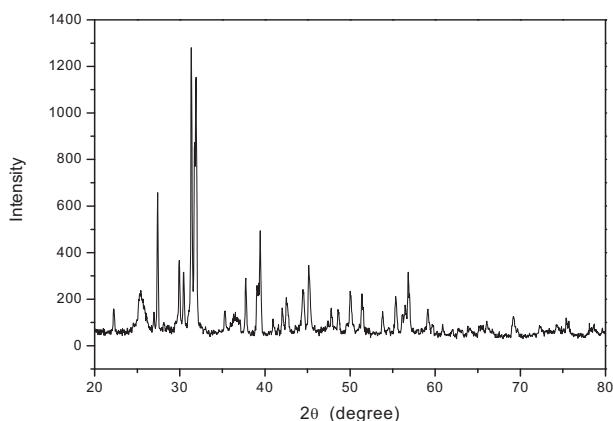


Figure 1: PXRD of  $\text{Sr}_{1.99}\text{Eu}_{0.01}\text{SiO}_4$  nanophosphor

From the full width at half maximum of the diffraction peaks the average crystalline size is calculate using the Debye-scherrer formula [15],

$$D = \frac{0.9 \lambda}{\beta \cos \theta} \quad \dots\dots\dots (1)$$

Where  $D \rightarrow$  average grain size of the crystallite,  $\lambda \rightarrow$  incident wavelength,  $\theta \rightarrow$  the bragg angle,  $\beta \rightarrow$  full width at half maxima. The grain size was found to be in the range of 35-45 nm.

### *Fourier Transform Infrared Spectroscopy (FTIR)*

The molecular structure of Eu doped  $\text{Sr}_2\text{SiO}_4$  was analyzed by FTIR. Fig 2 shows the FTIR spectra of  $\text{Sr}_2\text{SiO}_4$ : Eu phosphor powder. The absorption band at  $1481 \text{ Cm}^{-1}$  is ascribed to Sr-O stretching vibration. Si-O stretching [ $\text{F}_2(\nu_3)$ ] vibrations occur at the range of  $900\text{-}970 \text{ Cm}^{-1}$  and Si-O bending [ $\text{F}_2(\nu_4)$ ] vibration is observed at  $502 \text{ Cm}^{-1}$ . The absorption peak at  $3428 \text{ Cm}^{-1}$  is due to H-OH bond vibration of absorbed water [16].

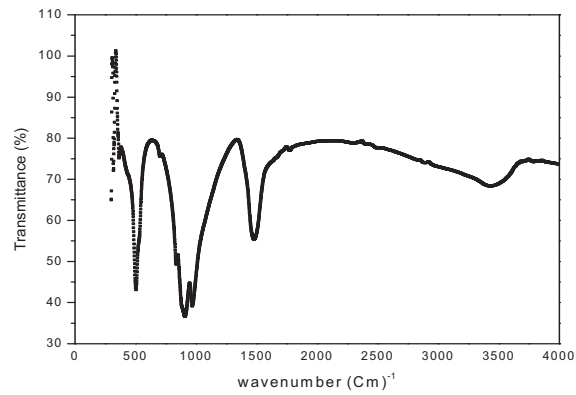


Figure 2 FTIR spectra of  $\text{Sr}_2\text{SiO}_4:\text{Eu}$  nanophosphor calcined at  $1100^\circ\text{C}$  for 3hr

### Scanning Electron Microscopy (SEM)

The surface morphology of  $\text{Sr}_2\text{SiO}_4:\text{Eu}$  nanophosphor prepared using citric acid as a fuel was studied using SEM. The results are shown in Fig 3. It can be clearly observed from these images that the powder show highly porous many agglomerates with an irregular morphology. This type of appearance is expected in combustion synthesis because of escape of large amount of gases. Large voids are also observed.

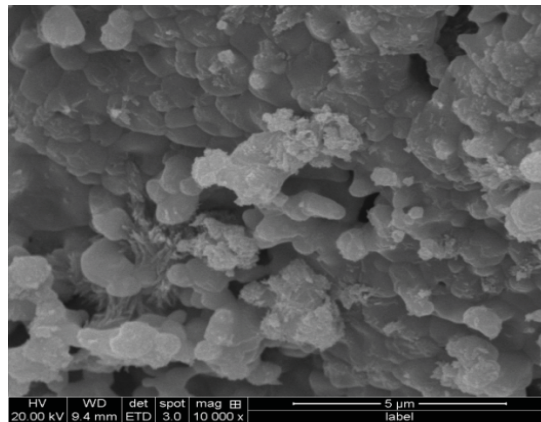


Figure 3 SEM images of  $\text{Sr}_2\text{SiO}_4:\text{Eu}$  nanophosphor

UV-Vis spectroscopy

UV-Vis spectroscopy has been used to study the absorption characteristics of Sr<sub>2</sub>SiO<sub>4</sub>: Eu. In order to know the sharper and prominent absorption the peaks were deconvoluted using origin software. The maximum absorption bands arise at 205, 226, 273 and 445 nm.

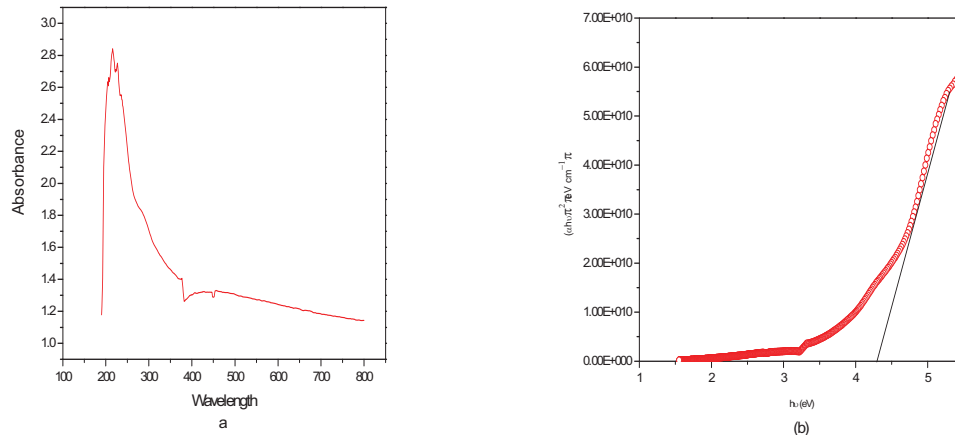


Figure 4 (a) UV-Vis spectra and (b) Band gap of Sr<sub>2</sub>SiO<sub>4</sub>: Eu<sup>3+</sup> nanophosphor

An intense absorption bands observed around 200- 300 nm which corresponds to oxygen to silicon (O-Si) ligand to metal charge transfer in the SiO<sub>3</sub><sup>2-</sup> group. The broad band's in the range 300-500 nm are attributed to the intra configurational 4f-4f transitions from the ground <sup>4</sup>F<sub>0</sub> level, which corresponds to the excitation spectra [17].

The optical band gap energy of Eu doped Sr<sub>2</sub>SiO<sub>4</sub> are estimated using the Tauc relation [18]

$$\alpha(h\nu) \sim (h\nu - E_g)^k \dots\dots\dots (2)$$

Where hν is energy of a photon and 'α' is the optical absorption co-efficient near the fundamental edge. The values of band gap can be obtained by plotting (αE)<sup>k</sup> v/s E in the high absorption end followed by extrapolating the linear region of the plot to (αE)<sup>k</sup>=0. The optical band gap value was found to be 4.35 eV.

### Photoluminescence (PL)

Figure 5 and 6 shows the excitation and emission spectra of  $\text{Sr}_2\text{SiO}_4:\text{Eu}$ . The excitation spectra recorded at 613 nm emission shows peak around 361 nm is due to charge transfer band between  $\text{O}^{2-}-\text{Eu}^{3+}$ . The electron transfers to partially filled 4f orbit of  $\text{Eu}^{3+}$  from 2p full orbit. This transfer leads to oxidation of  $\text{O}^{2-}$  to  $\text{O}^-$  and reduction of  $\text{Eu}^{3+}$  to  $\text{Eu}^{2+}$ . Thus the phosphor can be efficiently excited by mercury lamp [12]. Peaks at 376, 382, and at 393 nm are due to  ${}^7\text{F}_0 \rightarrow {}^5\text{G}_2$ ,  ${}^7\text{F}_0 \rightarrow {}^5\text{G}_5$  and  ${}^7\text{F}_0 \rightarrow {}^5\text{L}_6$  respectively.

In  $\text{Eu}^{3+}$  there are two types of excitation charge transfer band and 4f-4f transition. The filled  ${}^5\text{S}_2$  and  ${}^5\text{P}_6$  orbital shield the 4f orbital. Thus the influence on the optical transition by host lattice within the  $4\text{f}^n$  configuration is small and 4f-4f transition is sharp lines [3].

The emission spectrum was recorded with 393 nm excitation. The peaks in the emission spectra are due to  ${}^5\text{D}_0 \rightarrow {}^7\text{F}_j$  ( $j=1, 2, 3, 4\dots$ ). Major peaks are observed in red region. The peaks at 589-593, 613-619 and 702 nm are due to radiative transitions from  ${}^5\text{D}_0 \rightarrow {}^7\text{F}_1$ ,  ${}^5\text{D}_0 \rightarrow {}^7\text{F}_2$ ,  ${}^5\text{D}_0 \rightarrow {}^7\text{F}_4$ .

Broad band along with small peak appears around 431 nm in the blue region. It may be speculated that both couples (593 and 613 nm) corresponds to the  $\text{Eu}^{3+}$  emission. The couple arises due to  ${}^5\text{D}_0 \rightarrow {}^7\text{F}$  transition level at 393 nm characteristic excitation of  $\text{Eu}^{3+}$  ion.  $\text{Eu}^{3+}$  ion substitutes  $\text{Sr}^{2+}$  ions in the host lattice which may lead to emission at 593 and 613 nm [19].

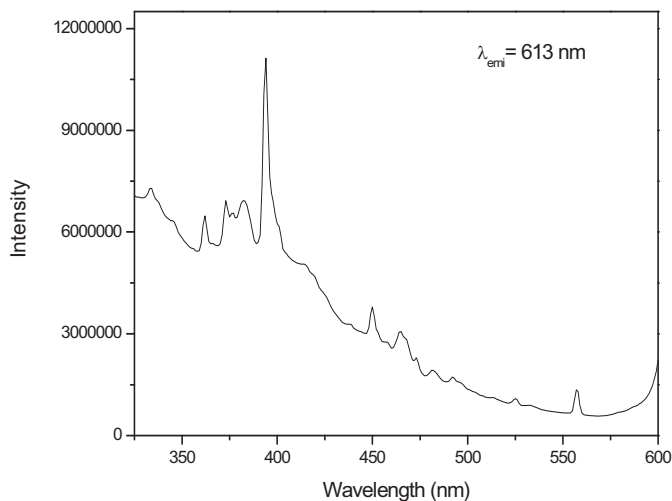


Figure 6 PL excitation spectrum of  $\text{Sr}_2\text{SiO}_4:\text{Eu}^{3+}$  nanophosphor

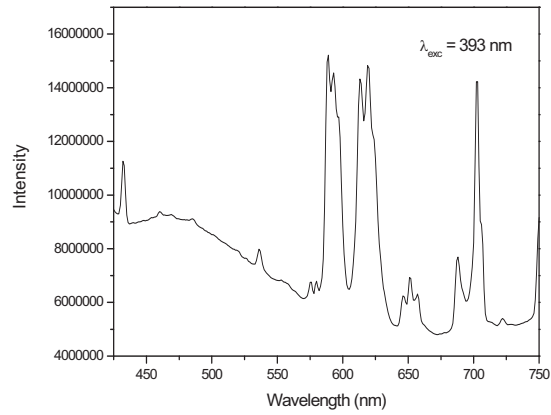


Figure 5 PL emission spectrum of  $\text{Sr}_2\text{SiO}_4: \text{Eu}^{3+}$  nanophosphor

### Thermoluminescence (TL)

The TL glow curves at a heating rate of  $5^\circ\text{C/s}$  from 1-6 Kgy of  $\gamma$ - irradiated  $\text{Sr}_2\text{SiO}_4: \text{Eu}$  nanophosphor synthesized by solution combustion method is as shown in the Figure 7. The single peak around  $173^\circ\text{C}$  was recorded.

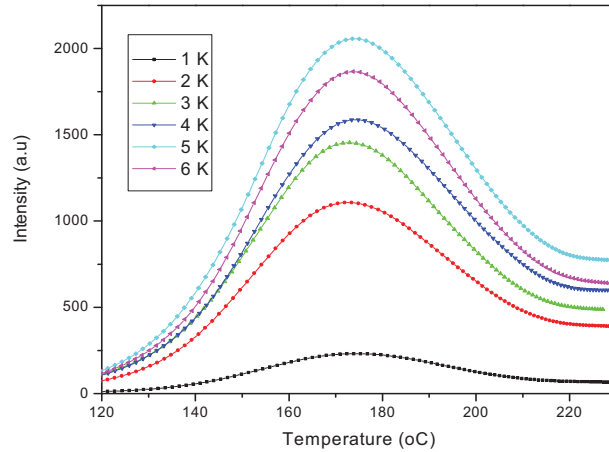


Figure 7 TL glow curves exposed in the  $\gamma$ -dose range of 1-6Kgy

However with increase in the  $\gamma$  dose the intensity goes on increases and becomes maximum for 5 KGy after that it decreases. The variation in glow peak intensity is mainly attributed to the trapping of electron and recombination efficiency depending on the irradiation given to it [20-21].

Further the increase in TL intensity is explained on the basis of Track Interaction Model. According to this model the number of traps generated due to irradiation depends on the length of tracks and cross section of the tracks in the matrix. Compared to microcrystalline materials in nanomaterials the length of such a track may be few tens of nanometers. Thus the creation of trap centers is very less for lower doses. However with further increase in dose more over lapped track occurs that may not respond and give rise to extra TL. Thus the decrease in intensity is due to overlapping tracks [22].

TL glow curve analysis leads to the estimation of localized trap depth. The analysis also leads to the estimation of kinetic parameters, E (measure of the energy required to eject an electron from the defect centre to the conduction band), s (rate of electron ejection), b (measure of the probability that a free electron gets retrapped) using chen's set of equation.

For the evaluation of kinetic parameters the glow curve was deconvoluted using origin 8.1 software. The kinetic parameters of deconvoluted glow curves are calculated using chens set of equation by modified peak shape method [23]

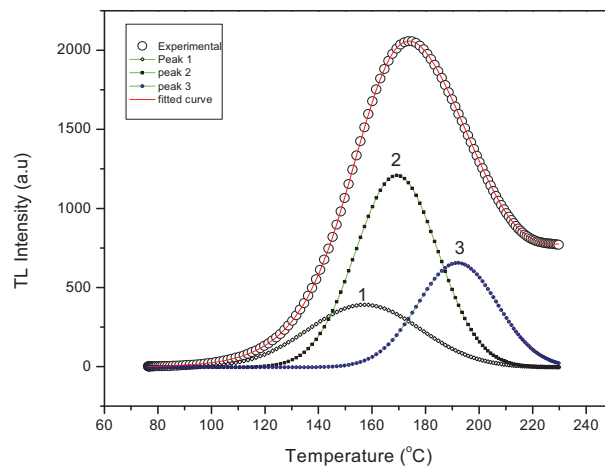


Figure 8 Glow curve deconvolution of  $\text{Sr}_2\text{SiO}_4:\text{Eu}$  nanostructure exposed to 5KGy dose at a heating rate of  $5^\circ\text{C/s}$



We have investigated the effect of different heating rates on the TL glow curves figure shows the TL glow curve at different heating rates with increase in heating rate the glow peak shifts towards higher temperature and TL intensity reduces which is due to well known phenomenon of thermal quenching [23].

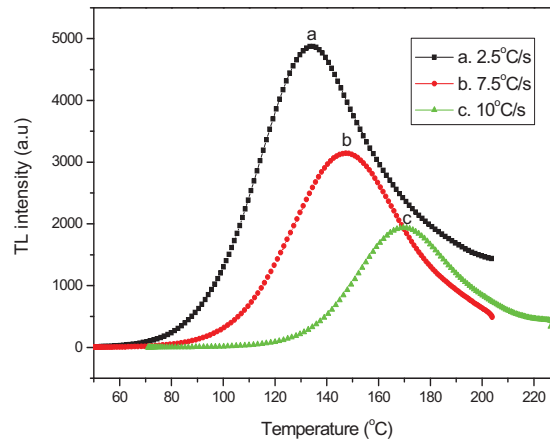


Figure 9 Effect of different heating rates on TL response of  $\text{Sr}_2\text{SiO}_4:\text{Eu}$

Thermal quenching was understood to be due to the increase probability of non radiative transitions competing with the radiative transitions. The increase in heating rate results in an increase in the temperature of glow peak thus shift in temperature was held responsible for the increase in the contribution of non radiative transitions [22]. Other than this the heating rate makes the migration of charge carriers during the TL read out

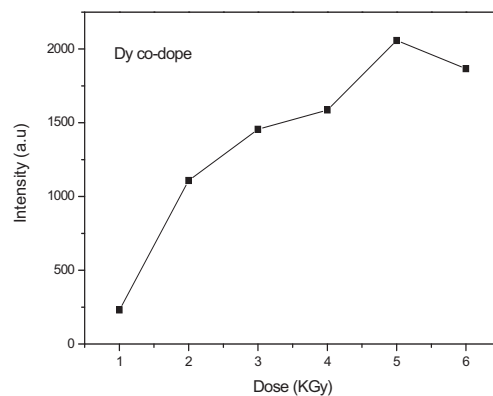


Figure 10 Variation of TL intensity of the TL peaks with the dose in the range (1-6KGy)

Table -1 Experiment Result

	Tm	$\mu\text{g}$	Order of kinetics	Activation energy (eV)			Average energy (eV)
				$E\tau$	$E\delta$	$E\omega$	
Peak 1	151.4	0.49	2	0.962	0.98	0.98	0.974
Peak 2	169	0.5	2	1.48	1.45	1.46	1.46
Peak 3	192.4	0.49	2	1.63	1.62	1.64	1.63

Table 1 The kinetic parameters for  $\text{Sr}_2\text{SiO}_4:\text{Eu}^{3+}$  phosphors estimated from Chen's glow peak shape method.

#### IV CONCLUSION

$\text{Eu}^{3+}$  (1 mol%) doped  $\text{Sr}_2\text{SiO}_4$  nanophosphor has been successfully synthesized by a low temperature solution combustion method using citric acid as a fuel. PXRD confirms that the nanophosphor attaining an orthorhombic structure without any secondary phase. SEM micrographs of the nanophosphor shows highly porous with large void and agglomeration. From UV -Vis studies the maximum absorption at 200-270 nm can arise due to transition between valence and conduction band. The  $\text{Sr}_2\text{SiO}_4:\text{Eu}^{3+}$  exhibits the maximum red emission along with emission in blue and green region. TL properties of  $\gamma$ - irradiated nanophosphor was investigated which shows a single peak at  $173^\circ\text{C}$ . It is observed that the intensity of glow peak increases linearly with the dose which indicates that the  $\text{Sr}_2\text{SiO}_4:\text{Eu}^{3+}$  is suitable for radiation dosimetry application.

## REFERENCES

- [1] G .Ramakrishna, .H .Nagabhushana, S.C. Prashantha, S.C. Sharma, B.M.Nagabhushana, “Role of flux on morphology and luminescence properties of  $\text{Sm}^{2+}$  doped  $\text{Y}_2\text{SiO}_5$  nanopowders for WLEDs” *Spectro Chemica Acta Part A; Molecular and Bio molecular Spectroscopy* 136, 356-365, (2015).
- [2] V. Gan, 2004. “*Nanostructures and Nanomaterials –Synthesis, properties and applications*”, Imperial college press: London,
- [3] QIAO Yanmin, ZHANG Xinbo, YE Xiao, CHEN Yan, GUO Hai. , “Photoluminescent properties of  $\text{Sr}_2\text{SiO}_4:\text{Eu}^{3+}$  and  $\text{Sr}_2\text{SiO}_4:\text{Eu}^{2+}$  phosphors prepared by solid state reaction method. *Journal of rare earths*, 27, 323, (2009).
- [4] D.V.Sunitha, H.Nagabhushana , Fouran singh, B.M. Nagabhushana, S.C.Sharma, R.P.S. Chakradar, “Thermo, ion and photoluminescence properties of 1000MeV  $\text{Si}^{7+}$  ions bombarded  $\text{CaSiO}_3:\text{Eu}^{3+}$  nanophosphor”. *Journal of luminescence*. (2012).
- [5] Wei-Hsiang Hsu, Meng Huei Sheng, Ming-Shyong. “Preparation of Eu activated strontium orthosilicate phosphor by a sol-gel method and its luminescent properties”. *Journal of alloys and compounds*, 467, 491-495, (2009).
- [6] J.S.Kim, P.E.Jeon, J.C. Choi, H.L.Park, “Emission color variation of  $\text{M}_2\text{SiO}_4:\text{Eu}^{2+}$  (M=Ba, Sr, Ca) phosphor for light –emitting diode”. *Solid state communication*, 133, 187-190, (2005).
- [7] E.D.Bacce, A.M. Pires, M.R. Davolor, “Influence of  $\text{Zn}^{2+}$  co-doping ion on  $\text{Eu}^{3+}$  -O $^{2-}$  associate luminescence in  $\text{Sr}_2\text{SiO}_4$ ”. *Journal of alloys and compounds*, 344, 312-315, (2002).
- [8] A.Jaganatha Reddy, M.K.Kokila, H.Nagabhushana, S.C.Sharma, J.L.Rao, C.Shivakumara, B.M.Nagabhushana, R.P.S. Chakradar, “Structural, EPR, photo and thermoluminescence properties of  $\text{ZnO}:\text{Fe}$  nanoparticles”. *Materials chemistry and Physics*, 133, 876-865, (2012).
- [9] Kyeong Youl Jung, Joo Hyun kim, Yun chang Kang, “ Luminescent Enhancement of Eu doped calcium magnesium silicate blue phosphor for UV-LED application” *Journal of luminescence*, 129, 615-619, (2009).
- [10] SUN Xiaoyuan, ZHANG Jiahua, ZHANG Xia, LUO Yongshi, WANG Xiaojun, “A green –yellow emitting  $\beta\text{-Sr}_2\text{SiO}_4:\text{Eu}^{2+}$  phosphor for near ultraviolet chip white light emitting diode”. *Journal of rare earths*, 26, 421, (2008).
- [11] Zhongra, Gou, Jiang chang,” Synthesis and in vitro bioactivity of dicalcium silicate powders”, *Journal of the European ceramics society*, 24, 93-99, (2004).
- [12] YU Quanmao, LIU Yufeng, WU Shan, LU Xingdong, HUANG Xinyang, LI Xiaoxia. “Luminescent properties of  $\text{Ca}_2\text{SiO}_4:\text{Eu}^{3+}$  red phosphor for trichromatic white light emitting diodes”. *Journal of rare earths*, 26, 783, (2008).
- [13] V.B.Bhatkar, S.K.Omanwar, S.V. Moharil, “Combustion synthesis of silicate phosphors”. *Optical materials*, 29, 1666-1750, (2007).
- [14] Shanshan Yao, Donha Chen.” Combustion synthesis and luminescent properties of a new material  $\text{Li}_2(\text{Ba}_{0.99}\text{Eu}_{0.01})\text{SiO}_4:\text{B}^{3+}$  for ultraviolet light emitting diodes” *Optics and laser technology*, 40, 466-471, (2008).
- [15] A.,Jaganatha Reddy, M.K.Kokila, H.Nagabhushana, J.L.Rao, C.Shivakumara, B.M.Nagabhushana, R.P.S. Chakradhar, “Combustion synthesis, characterization and Raman studies of  $\text{ZnO}$  nanopowder”. *Spectra chemical acta part A*, 81, 53-58, (2011).
- [16] M.Handke, and M. Urban, “IR and Raman spectra of alkaline earth metals orthosilicates”. *Journal of molecular structure*, 79, 353-356, (1982).
- [17] N .Dhananjaya, H. Nagabhushana, B.M. Nagabhushana, B. Rudraswamy, C. Shivakumara, K.P.Ramesh, R.P.S Chakradhar,. “ Thermo and photoluminescence properties of  $\text{Eu}^{3+}$  activated hexagonal, monoclinic and cubic gadolinium oxide nanorods” *Physica B*, 406, 1645-1652, (2011).
- [18] J.Tauc, In:F Abeles (Ed) , 1970 “*Optical properties of solid*”s, north Holland publishers, Amsterdam.
- [19] I.M.Nagpure, Subhajit Saha, S.J. Dhoble, “Photoluminescence and thermoluminescence characterization of  $\text{Eu}^{3+}$  and  $\text{Dy}^{3+}$  activated  $\text{Ca}_3(\text{PO}_4)_2$  phosphor”. *Journal of luminescence*, 129, 898-905, (2009).
- [20] K.S.Chung, H.S.Choe, J.I. Lee, J.L. Kim, “A new method for the numerical analysis of thermoluminescence glow curve”. *Radiation measurements*, 42, 731-734, (2007).
- [21] M.Chandrasekhar, D.V.Sunitha, N.Dhananjaya, H.Nagabhushana, S.C.Sharma, B.M.Nagabhushana, C.Shivakumara, R.P.S, Chakradhar, “Thermoluminescence response in gamma and UV irradiated  $\text{Dy}_2\text{O}_3$ ”. 132, 1798-1806, . (2012),
- [22] Vural E Kafadar, “Thermal quenching of thermoluminescence in TLD-200, TLD-300 and TLD-400”. *Physica B*, 406, 537-540, (2011).
- [23] N.Dhananjaya, H.Nagabhushana, B.M.Nagabhushana, B.Rudraswamy, C.Shivakumara, K.P, Ramesh, R.P.S. Chakradhar, “Thermo and photoluminescence properties of  $\text{Eu}^{3+}$  activated hexagonal, monoclinic and cubic gadolinium oxide nanorods”. *Physica B*, 406, 1645-1652, (2011).